MEMS-Based Channelized Dispersion Compensator With Flat Passbands

David T. Neilson, *Senior Member, IEEE, Member, OSA*, Roland Ryf, *Member, IEEE*, Flavio Pardo, Vladimir A. Aksyuk, Maria-Elina Simon, Daniel O. Lopez, Dan M. Marom, *Member, IEEE*, and S. Chandrasekhar, *Fellow, IEEE*

***Abstract*—This paper describes a continuously variable and independently addressable channelized dispersion compensator. The optical system is a free-space grating-based system used in a four-pass configuration to ensure flat passbands. The variable dispersion is produced by an array of thermally adaptable curvature micromechanical mirrors. A per-channel variable dispersion greater than +/−400 ps/nm has been demonstrated, with 58 GHz +/−0.4 dB flat passband on 85 GHz spacing. The group delay ripple is less than 7 ps and the penalty with 40 Gb/s CSRZ is 0.7 dB.**

***Index Terms*—Dispersion compensator, microelectromechanical systems (MEMS).**

I. Introduction

THE importance of dispersion control in optical transmission systems has grown with increasing data rates. The high precision required in setting dispersion compensation, will mean that active dispersion compensation is necessary to overcome limitations in accurately setting the dispersion when building a system and environmental factors during the life of the system. Additionally, the desire to provide reconfigurable routes in the optical domain has also driven the need for dynamic dispersion compensation, since the optical paths are not fixed, but can vary by channel. Thus, the necessity of providing dynamic per-channel dispersion compensation has made it a critical technology for the evolution of lightwave communications.

While there are several approaches to dynamic dispersion compensation including fiber, waveguide, and bulk optics, the mechanism for creating the wavelength dependent group delay can be placed in two categories. The first category employing multipath interference such as fiber Bragg gratings [1], waveguide ring resonators [2], and free-space Gires-Tournois interferometers [3]–[5]. The second category uses grating-based systems with a variable phase element at an image plane to produce beam displacement on the grating causing variable group delay, such as the bulk optics virtual image phased array [6], microelectromechanical systems (MEMS) image plane phase shifter [7], a liquid crystal phase shifter [8], or waveguide grating routers with a thermooptic lens [9].

Manuscript received July 3, 2003; revised October 17, 2003.

D. T. Neilson, R. Ryf, D. M. Marom, and S. Chandrasekhar are with Bell Laboratories, Lucent Technologies, Holmdel, NJ 07733 USA (e-mail: neilson@lucent.com).

F. Pardo, V. A. Aksyuk, M.-E. Simon, and D. O. Lopez are with Bell Laboratories, Lucent Technologies, Murray Hill, NJ 07974 USA.

Digital Object Identifier 10.1109/JLT.2003.822835

The optical system described in this paper uses the latter grating-based approach with the variable curvature MEMS mirror as the image plane phase shifting element. However, this design has two major advantages over previous devices. First, since it does not use an echelle grating, it can utilize an array of MEMS mirrors with variable curvature and, therefore, can provide differing dispersion on each of the channels in the system. This allows it to simultaneously compensate a multichannel system with arbitrary dispersions. Second, it uses an optical configuration with four passes on the grating, which allows the device to have flat passbands. Four pass systems have previously been considered for pulse compressors [10], [11] but the optical configurations only partially flatten the passband.

Since the grating-based designs are nonminimum phase filters [12], we know that the Hilbert transform may not be used to infer the phase response from the amplitude. Thus, it is possible in principle to obtain dispersion without creating amplitude variations. The origin of the change in passbands with dispersion in the previous systems [6]–[9] is that they use the second pass of the grating to provide both the wavelength delay and the wavelength recombination. Doing both in a single stage is incompatible with flat passbands since delay requires the beam be displaced on the grating, while a flat wavelength passband requires that for all the wavelengths the beams come from the same pupil position. The solution for flat-passbands is to separate these functions by using four grating passes, one to disperse, two to delay and the last to recombine the spectrum. In addition to flattening the passband, the four-pass system produces twice the group delay and hence dispersion of a conventional two-pass system, because the light double passes the grating system producing the group delay.

II. System Design

The system consists of a folded 4f dispersive imaging system, a 1D array of MEMS mirrors and beam forming and reflection module. The dispersive system, shown schematically in Fig. 1, consists of a 50-mm focal length lens [13] in conjunction with an 1800 gr/mm prism (BK7) buried grating (1265 gr/mm equivalent) [14]. The grating has a high efficiency (∼0.9 dB loss per pass) for a single polarization, which helps to reduce the four-pass loss, but requires us to use aperture division polarization diversity [13], [15]. An array of thermally actuated, variable curvature, MEMS mirrors, shown in Fig. 2, is placed at the image plane. The mirrors are composed of a stressed gold

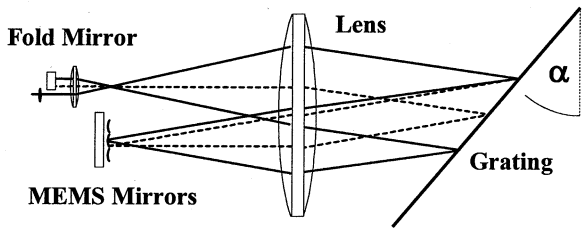

Fig. 1. Schematic of system showing path taken by light at the center of the channel (solid) and light at the edge of the channel (dash).

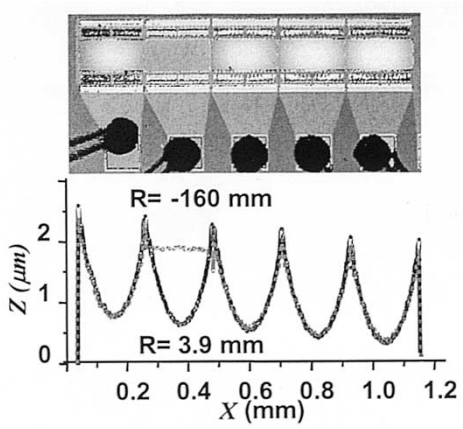

Fig. 2. MEMS mirror array showing five thermally actuated mirrors on a 210 μm pitch. Graph illustrates starting and partially actuated curvature of the second mirror (20 mA, 10 V).

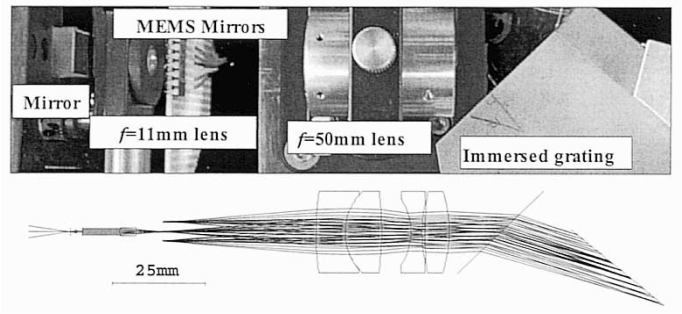

Fig. 3. Layout of system showing folding mirror, condenser lens ($\mathrm{f} = 11$ mm), MEMS devices, relay lens ($\mathrm{f} = 50$ mm) and immersed grating (1800 gr/mm). A ray trace of the system for wavelengths from 1542 to 1558 nm is shown on the lower half.

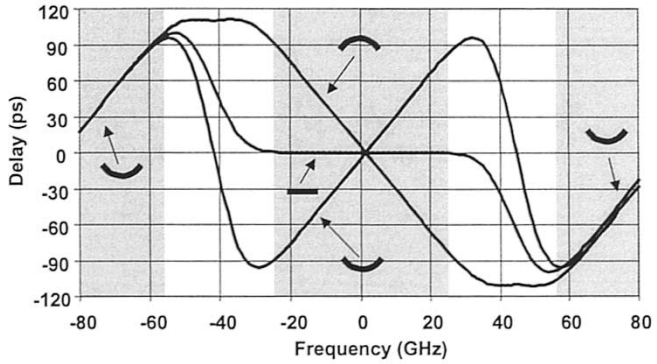

Fig. 4. Calculated group delay passbands of device with 68 μm diameter beams and 210 mm spaced mirrors. The channel spacing is 85 GHz and the linear group delay region is 50 GHz.

film on silicon, and start with a negative curvature of radius 3.9 mm. They are heated by use of individual resistance heaters in each mirror. When heated they deform to produce a range of curvatures through flat up to a positive curvature of radius 3.9 mm. While not optimal for the final application these mirrors allow demonstration of the subsystem concept. Thermally actuated mirrors have relatively large power dissipations and induce some curvature in adjacent mirrors. Additionally the increased temperature of operation will tend to accelerate aging and metallic creep issues [16].

Light enters the system, via a circulator on a fiber and is formed into a beam by a collimator ($f = 1.7$ mm). A birefringent beam walk off crystal and a half-wave-plate produce polarization diversity beams. The beams then pass through a ($f = 11$ mm) condenser lens and enter the dispersive imaging system, shown in Fig. 3. The two emerging beams of light pass through the condenser and 50 mm lens to produce a 1.7 mm $1/\mathrm{e}^2$ beam diameter on the grating, where they are spatially dispersed and imaged by the 50 mm lens onto the MEMS mirror array. The $1/\mathrm{e}^2$ beam diameter at the MEMS device is 68 μm. The mirrors are 210 μm long corresponding to a channel spacing of 0.67 nm or 85 GHz. The curvature of the MEMS mirrors redirects different spectral components of each channel to different places on the grating.

The light passes through the 50-mm lens and the condenser to hit a plane mirror, adjacent to the beams entering the system, which retroreflects the beam back through the collimator and dispersive system to the MEMS mirror, where the angular shift induced by the curvature is undone by a second reflection off the MEMS mirror. The light is then recombined by the lens and grating and coupled into the original fiber where the circulator separates the light to the output port. The overall system shown in Fig. 3 is 150 mm long × 40 mm × 40 mm. We would expect a 1-dB amplitude passband of around 74 GHz. The group delay passbands are expected to be narrower, as shown in Fig. 4, with flat dispersion expected over 50 GHz and maximum to minimum delay width of 58 GHz.

The system was operated with five MEMS mirrors spanning 3.5 nm, but the optics is capable in its current form of supporting 16 nm or 20 100-GHz spaced channels, shown in the ray trace of Fig. 3, with negligible increase in insertion loss.

The insertion loss has the following anticipated contributions: 3.6 dB from four passes of the grating; 1.5 dB from coating losses of eight passes of the four-element $f = 50$ mm lens; 0.5 dB from coupling losses due to aberration; 1.2 dB from the circulator; 0.5 dB from the polarization diversity optics; 0.3 dB from the reflectivity of the MEMS mirror. This gives an expected loss of 7.6 dB for the system.

The group delay per pass of a grating system in Littrow configuration where α is the grating angle is $(2.f.tan\theta.tan\alpha)/c$ with θ as the deflection angle of the beam at the image plane, f is the focal length of the lens, and c is the speed of light. In a system with a MEMS mirror curvature of C_R, and a beam coming from a distance Δd from the center of the curved MEMS

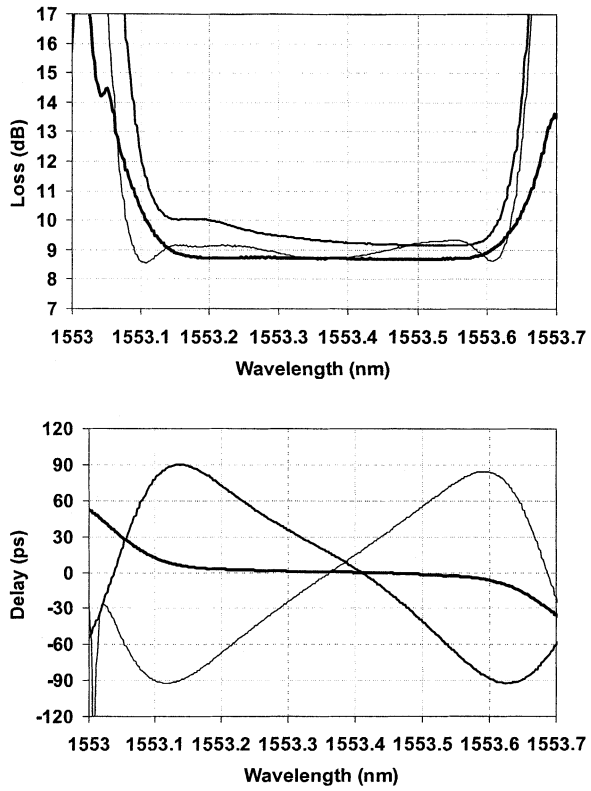

Fig. 5. The loss and group delay of the device as the curvature is varied. Dispersion of $+/-410$ ps/nm is achieved over a 0.4-nm bandwidth. The passband has less than $+/-0.4$ dB ripple over the 0.45-nm bandwidth.

mirror the local mirror slope is ΔdC_R, and the resulting deflection angle of the beam θ is given by $tan\theta = 2\Delta dC_R$. Thus, for the four-pass system, the group delay is

$$\tau = \frac{8f\Delta d C_R \tan\alpha}{c}. \tag{1}$$

For constant curvature, this gives a delay proportional to the curvature and displacement of the beam from the center of the curved mirror. The spatial dispersion of the system at the curved mirror is $\Delta d/\Delta\lambda = 2f\tan\alpha/\lambda$. Thus, the dispersion is

$$CD = \frac{16f^2 C_R \tan^2\alpha}{\lambda c} \tag{2}$$

and is proportional to curvature of the curved mirror and the square of the spatial spectral dispersion of the optical system. For $f = 50$ mm, $\alpha = 78°$, $\lambda = 1.55$ μm, and C_R in mm^{-1}, we obtain a nominal CD $= 1900C_R$ ps/nm.

III. Experimental Results

The measured the loss and dispersion for various actuated curvatures of the MEMS mirrors are shown in Fig. 5. We observe that the passbands are generally flat, though there is some slight narrowing with curvature, which is caused by residual aberrations of the optical system. For a curvature of 3.9 mm, we obtained a maximum 187 ps delay over a 0.5-nm passband (58 GHz) and a uniform dispersion of 410 ps/nm over 0.4-nm band (50 GHz) which is consistent with the expected bandwidth. With curvature of -3.9 mm, we obtain 192 ps delay over a 0.5-nm passband giving a uniform dispersion of -410 ps/nm over 0.4 nm. The passband is flat to within $+/-0.4$ dB across these bandwidths and dispersions. There is a slight variation in the insertion loss as a function of the curvature, due to curvature of the MEMS mirrors in the nondispersion direction and higher-order aberrations of the system, with up to 1 dB more loss at the higher dispersions. The measured loss of 8.7 dB is slightly greater than the anticipated loss of 7.6 dB and the excess may be related to curvature of the MEMS mirror in the nondispersion direction and nonoptimal alignment of the system.

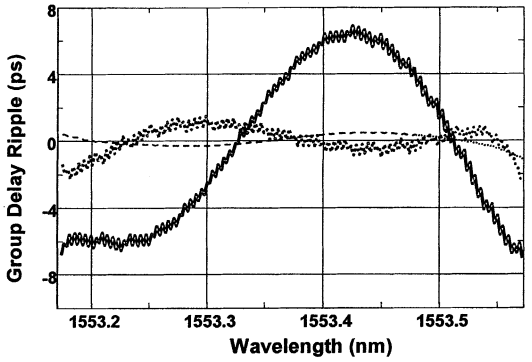

Fig. 6. Group delay ripple for dispersion values of 404 ps/nm (dot), -15 ps/nm (dash) and -386 ps/nm (solid).

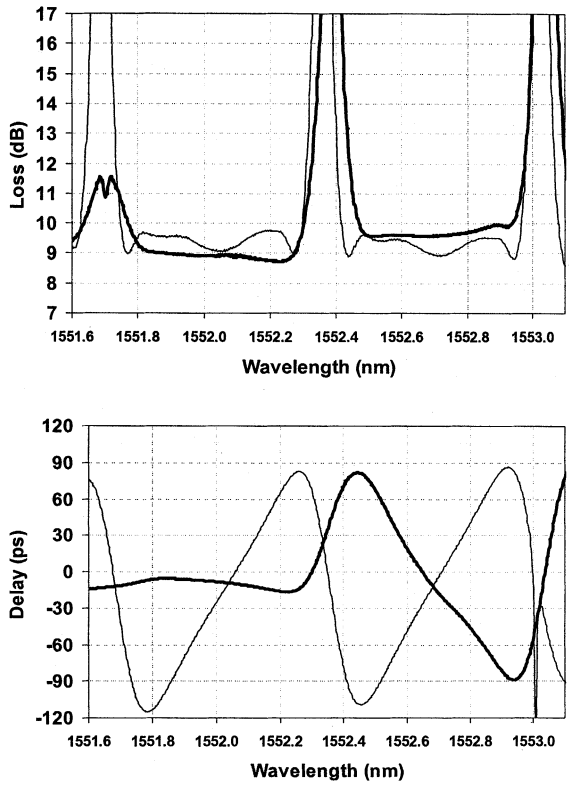

Fig. 7. Loss and dispersion on adjacent channels, for two states. Adjacent channels with the same dispersion 440 ps/nm (thin) and one with near zero (<20 ps/nm) while the neighbor has -410 ps/nm (heavy).

A significant characteristic of any dispersion compensator is the amount of group delay ripple that it produces. We have measured this for a variety of dispersion values and the results are shown in Fig. 6 for a 0.4 nm width (50 GHz). The mirrors when unheated and when heated up to flat produce a group delay

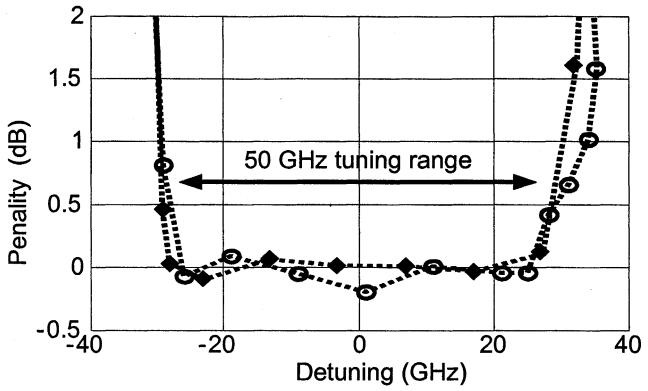

Fig. 8. Passband for 10 Gb/s NRZ when compensating dispersions of 0 (open symbols) and −332 ps/nm (closed symbols).

ripple of less than $+/-2$ ps. Beyond this they start to exhibit group delay ripple increasing to $+/-7$ ps at maximum dispersion. The asymmetry in the ripple can be attributed to nonuniformity of thermally induced curvature in these experimental mirrors.

A distinct advantages of this device is that it can have different dispersions on adjacent channels, as is illustrated by the results in Fig. 7, which shows adjacent channels with similar and dissimilar dispersions.

The polarization dependent loss is around 0.3 dB and there is 5 ps GVD from the design of polarization diversity optics, which could be reduced upon further redesign. Tests of the device with 10 Gb/s NRZ PRBS $2^{31}-1$, indicate no transmission penalties other than from the dispersion. We find penalty free operation at 10 Gb/s over a 50-GHz passband both at zero dispersion and when compensating −332 ps/nm dispersion, as shown in Fig. 8, consistent with the 58-GHz measured passbands.

We have also tested the device with 40 Gb/s CSRZ PRBS $2^{31}-1$, and we find that the dispersion compensator produces 0.7 dB penalty when compensating a fiber with −348 ps/nm. There is a $+/-5$ GHz window for 40 Gb/s CSRZ that is consistent with the 58 GHz passband.

IV. Summary

We have proposed and demonstrated a new optical configuration for a dispersion compensator. The new design allows for flat passbands across a wide range of dispersion. Since the four-pass configuration also provides more dispersion than previous double pass systems, it enables the use of nonechelle grating technologies. These gratings allow the individual channels to be compensated separately by the array of MEMS mirrors. This system has demonstrated individual channel dispersion compensator with flat passbands and greater than $+/-400$ ps/nm of dispersion, with less than 10 dB insertion loss.

References

[1] B. J. Eggleton, A. Ahuja, P. S. Westbrook, J. A. Rogers, P. Kuo, T. N. Nielsen, and B. Mikkelsen, "Integrated tunable fiber gratings for dispersion management in high-bit rate systems," *J. Lightwave Technol.*, vol. 18, pp. 1418–1432, 2000.

[2] C. K. Madsen, G. Lenz, A. J. Bruce, M. A. Cappuzzo, L. T. Gomez, and R. E. Scotti, "Integrated all-pass filters for tunable dispersion and dispersion slope compensation," *IEEE Photon. Technol. Lett.*, vol. 11, pp. 1623–1625, 1999.

[3] D. J. Moss, M. Lamont, S. McLaughlin, G. Randall, P. Colbourne, S. Kiran, and C. A. Hulse, "Tunable dispersion and dispersion slope compensators for 10 gb/s using all-pass multicavity etalons," *IEEE Photon. Technol. Lett.*, vol. 15, pp. 730–732, May 2003.

[4] C. K. Madsen, J. A. Walker, J. E. Ford, K. W. Goossen, T. N. Nielsen, and G. Lenz, "A tunable dispersion compensating MEMS all-pass filter," *IEEE Photon. Technol. Lett.*, vol. 12, pp. 651–653, June 2000.

[5] K. Yu and O. Solgaard, "Tunable chromatic dispersion compensators using MEMS Gires-Tournois interferometers," in *IEEE/LEOS Int. Conf. Optical MEM's 2002 Conf. Dig.*, 2002, pp. 181–182.

[6] M. Shirasaki, "Chromatic-dispersion compensator using virtually imaged phased array," *IEEE Photon. Technol. Lett.*, vol. 9, pp. 1598–1600, 1997.

[7] T. Sano, M. Harumoto, T. Iwashima, T. Kanie, M. Katayama, M. Nishimura, M. Shigehara, and H. Suganuma, "Novel multi-channel tunable chromatic dispersion compensator based on MEMS & diffraction grating," in *Optical Fiber Communication Conf.*, 2003, pp. 722–723.

[8] A. M. Weiner, D. E. Leaird, J. S. Patel, and J. R. Wullert, "Programmable shaping of femtosecond optical pulses by use of 128-element liquid crystal phase modulator," *IEEE J. Quantum Electron.*, vol. 28, pp. 908–920, Apr. 1992.

[9] C. R. Doerr, L. W. Stulz, S. Chandrasekhar, L. Buhl, and R. Pafchek, "Multichannel integrated tunable dispersion compensator employing a thermooptic lens," in *Optical Fiber Communication Conf.*, 2002, postdeadline paper FA6-1.

[10] O. E. Martinez, "Design of high-power ultrashort pulse amplifiers by expansion and recompression," *IEEE J. Quantum Electron.*, vol. 23, pp. 1385–1387, 1987.

[11] M. M. Wefers and K. A. Nelson, "Space-time profiles of shaped ultrafast optical waveforms," *IEEE J. Quantum Electron.*, vol. 32, pp. 161–172, 1996.

[12] G. Lenz, B. J. Eggleton, C. R. Giles, C. K. Madsen, and R. E. Slusher, "Dispersive properties of optical filters for WDM systems," *IEEE J. Quantum Electron.*, pp. 1390–1402, Aug. 1998.

[13] D. M. Marom, D. T. Neilson, D. S. Greywall, V. Aksyuk, M. E. Simon, N. R. Basavanhally, P. R. Kolodner, Y. L. Low, F. Pardo, C. A. Bolle, C. S. Pai, D. López, J. A. Taylor, J. E. Bower, J. Leuthold, M. Gibbons, and C. R. Giles, "Wavelength selective 4 × 1 switch with high spectral efficiency, 10 dB dynamic equalization range and internal blocking capability," in *ECOC 2003*, Rimini, Italy, Sept. 21–25, 2003, Paper We4.P.130.

[14] *http://www. gratinglab. com/library/telecom/1800. pdf* [Online]

[15] D. M. Marom, D. T. Neilson, D. S. Greywall, N. R. Basavanhally, P. R. Kolodner, Y. L. Low, C. A. Bolle, S. Chandrasekhar, L. Buhl, S.-H. Oh, C. S. Pai, K. Werder, H. T. Soh, G. R. Bogart, E. Ferry, F. P. Klemens, K. Teffeau, J. F. Miner, S. Rogers, J. E. Bower, R. C. Keller, and W. Mansfield, "Wavelength selective 1 × 4 switch for 128 WDM channels at 50 GHz spacing," in *Optical Fiber Communication Conf. Exhibit (OFC 2002)*, 2002, pp. 857–859.

[16] H. R. Shea, S. Arney, A. Gasparyan, M. Haueis, V. A. Aksyuk, C. A. Bolle, R. E. Frahm, S. Goyal, F. Pardo, and M. E. Simon, "Design for reliability of MEMS/MOEMS for lightwave telecommunications," in *15th Annual Meeting IEEE Lasers and Electro-Optics Soc. (LEOS 2002)*, vol. 2, 2002, pp. 418–419.

David T. Neilson (M'96-SM'02) received the B.Sc. (Hons.) degree in physics and the Ph.D. degree in physics for work on optical nonlinearities in InGaAs quantum-well devices both from Heriot-Watt University, U.K., in 1990 in 1993, respectively.

From 1993 to 1996, he was a Postdoctoral Researcher with Heriot-Watt University, U.K., working with systems and devices for free-space optical interconnects. From 1996 to 1998, he was a Visiting Scientist with the NEC Research Institute, Princeton, NJ, researching optical interconnects for high-performance computing. In 1998, he joined Bell Laboratories, Holmdel, NJ, where he has worked on MEMS-based cross connects, wavelength selective switches, equalizers, and dispersion compensators. He is currently a Technical Manager with responsibility for optoelectronic device growth and fabrication facility. He has more than 80 publications in the field of optical interconnects and switching.

Dr. Neilson is a senior member of LEOS and a member of the OSA.

Roland Ryf (M'03) received the B.S. degree in electrical engineering from the Interstate University of Applied Sciences of Technology Buchs, Switzerland, in 1990, the M.S. degree in physics, and the Ph.D. degree in physics, while working on photorefractive self-focusing and spatial solitons, parallel optical processing based on holographic storage, and fast optical correlation, in 1995 and 2000, respectively.

Since May 2000, he has been with the Photonic Subsystem Department, Bell Laboratories, Lucent Technologies, Holmdel, NJ, where he is focusing on the optical design and prototyping of optical microelectromechanical system (MEMS)-based switches, spectral filters, and dispersion compensators, and the demonstration of their applications in optical networks.

Flavio Pardo, photograph and biography not available at the time of publication.

Vladimir A. Aksyuk, photograph and biography not available at the time of publication.

Maria-Elina Simon, photograph and biography not available at the time of publication.

Daniel O. Lopez, photograph and biography not available at the time of publication.

Dan M. Marom (S'98-M'01) received the B.Sc. degree in mechanical engineering and the M.Sc. degree in electrical engineering from Tel-Aviv University, Israel, in 1989 and 1995, respectively. He received the Ph.D. degree from the University of California, San Diego (UCSD), in 2000. In his doctoral dissertation, he investigated femtosecond rate optical signal processing with applications in ultrafast communications.

From 1996 through 2000, he was a Fannie and John Hertz Foundation Graduate Fellow at UCSD. In 2000, he joined the Advanced Photonics Research Department at Bell Laboratories, Lucent Technologies, Holmdel, NJ, where he is working on novel MEMS-based switching solutions using MEMS technology for optical communications.

Dr. Marom received the IEEE Lasers and Electro-Optics Society Best Student Paper Award in 1999 for his work describing instantaneous time reversal of complex amplitude ultrafast waveforms.

S. Chandrasekhar (M'89-F'01) was born in Tiruchirapalli, Tamil Nadu, India, on January 26 1952. He received the B.Sc., M.Sc., and Ph.D. degrees in physics from the University of Bombay, Bombay, India, in 1973, 1975, and 1985, respectively.

He joined the Tata Institute of Fundamental Research, Bombay, as a Research Scholar in 1975 and then became a Research Associate in 1979. He has been engaged in research on Si-SiO_2 interface studies, CMOS integrated circuits, ion implantation, charge coupled devices, and laser recrystallization. In 1986, he joined AT&T Bell Laboratories (now Bell Laboratories, Lucent Technologies), Crawford Hill Laboratory, Holmdel, NJ, as a Postdoctoral Member of Technical Staff. Since then, he has been working on III-V compound semiconductor devices for optoelectronic applications, primarily waveguides, photodetectors, heterojunction phototransistors, and bipolar transistors (HBTs). He became a permanent Member of Technical Staff in May 1992. He has been engaged in high-speed optoelectronic integrated circuits (OEICs), integrating p-i-n photodetectors and laser diodes with HBTs, for long wavelength optical communications. Since January 1999, he has been responsible for forward-looking research in WDM optical networking. He has set up an optical networking test-bed for investigation of optical networks comprising add/drop multiplexers, optical cross connects, and wavelength selective switching. His current interests include 40 Gb/s transport and networking, modulation formats, and electronic signal processing at the receiver. He holds 12 U.S. patents.

He is a member of the IEEE Electron Devices Society and the IEEE Lasers and Electro-Optics Society. He has been an Associate Editor of the IEEE PHOTONICS TECHNOLOGY LETTERS since 1998. He has been a member of the Technical Program Committees of the IEDM, the DRC, and the OFC conferences. He was recently awarded the IEEE LEOS Engineering Achievement for 2000 jointly with two other awardees for his contribution to OEIC photoreceivers.